DOI: 10.58895/ksp/1000044906-16 erschienen in:

OCM 2015 - 2nd International Conference on Optical Characterization of Materials, March 18th – 19th, 2015, Karlsruhe, Germany : Conference Proceedings

DOI: 10.58895/ksp/1000044906 | https://www.ksp.kit.edu/site/books/m/10.58895/ksp/1000044906/

Application of near-infrared (NIR) spectroscopy to sensor based sorting of an epithermal Au-Ag ore

M. Dalm,[1] M. W. N. Buxton[1] and F. J. A. van Ruitenbeek[2]

[1] Resource Engineering, Faculty of Civil Engineering and Geosciences, Delft University of Technology,
P.O. Box 5048, 2600 GA, Delft, The Netherlands

[2] Department of Earth Systems Analysis, Faculty of Geo-Information Science and Earth Observation (ITC), University of Twente,
P.O. Box 6, 7500 AA, Enschede, The Netherlands

Abstract Test work was performed with near-infrared (NIR) spectroscopy on 94 ore samples from a South-American Au-Ag mine. The aim of the test work was to investigate if alteration minerals can be detected with the NIR sensor that can be used as indicators of ore value. Partial least squares discriminant analysis (PLS-DA) was applied to the spectral data to make classification models that use the measured NIR spectra to distinguish samples with certain Au, S or C grades. This showed that detection of mineralogy with NIR spectroscopy can be used to discriminate on i) ore particles with low Au and Ag grades ii) ore particles with high carbon contents iii) ore particles with high sulphide contents.

1 Introduction

Sensor based sorting represents all applications where singular particles are mechanically separated on certain physical properties after determining these properties by a sensor. It can be incorporated as a pre-concentration step in ore processing operations to eliminate subeconomic ore material prior to conventional processing. This has potential to reduce the costs of processing mined materials [1–6]. Sensor types that are currently used with sensor based sorting include optical,

near-infrared, X-ray transmission, X-ray fluorescence and electromagnetic sensors [7, 8]. None of these sensors have been proven to be able to directly detect the Au content of epithermal Au ores.

Near-infrared (NIR) sensors used in sensor based sorting record the intensity of NIR radiation that is reflected from a solid material as a function of wavelength. NIR radiation is electromagnetic radiation, or light, with wavelengths ranging from 700 nm to 1 mm. Certain solid materials produce intense absorption of radiation around specific wavelengths in this region. This is caused by electronic molecular processes (crystal field effects, charge transfer, colour centres, conduction band transitions) and/or molecule bond vibrations [9, 10]. Identification of minerals is often possible by analysing the locations, shapes and relative intensities of all absorption features in the NIR spectrum of an ore particle. Not all minerals can be identified with NIR spectroscopy. It is restricted to minerals containing elements or molecule bonds that produce diagnostic absorptions. Minerals that that produce diagnostic absorptions are referred to as NIR active minerals.

Test work was performed to investigate the applicability of an NIR sensor to characterise epithermal Au-Ag ores on their economic value. The NIR sensor was selected because NIR spectroscopy has been proven to be a valuable tool in mapping the distribution of alteration minerals at epithermal ore deposits [11]. Deposition of Au and Ag at these deposits is related to the formation of specific alteration minerals [12–14]. It is therefore possible that the detection of alteration mineralogy with an NIR sensor can be used for predicting the economic value of the ore.

2 Hydrothermal alteration at epithermal ore deposits

Epithermal Au-Ag deposits are formed by hydrothermal activity that is driven by a magmatic intrusion occurring at several kilometres below the Earth's surface. Hydrothermal activity is the movement of hot aqueous (hydrothermal) fluids through the Earth's crust and interaction between these fluids and the rocks through which they pass. The hydrothermal fluids responsible for epithermal deposit formation originate from the magma and are released due to cooling of the magmatic intrusion [15]. Au, Ag and other elements are dissolved within these fluids as ions or complex ions. After release from the magma, the hy-

drothermal fluids flow towards the surface due to the relatively high pressure and temperature. The ascending magmatic fluids may subsequently mix with meteoric fluids which changes the fluid chemistry and temperature.

Epithermal Au-Ag deposits form at depths up to 1500 m below the surface and temperatures < 300 °C. Sharp pressure and temperature gradients in this environment results in boiling of the hydrothermal fluids, which changes fluid composition and forces Au and Ag to precipitate [13, 15]. The hydrothermal fluids that introduce Au and Ag in epithermal deposits also introduce, remove and/or redistribute other pre-existing components of the host rock. This is referred to as hydrothermal alteration [15]. Hydrothermal alteration results in the formation of alteration minerals. The type of alteration minerals that are formed depends on the pressure and temperature of the hydrothermal fluids and on the composition of both the hydrothermal fluids and the host rock [15]. Because precipitation of Au and Ag also depends on hydrothermal fluid properties, it is related to the formation of specific alteration minerals [12–14].

3 Sorting objectives of the test work

Test work was performed to investigate the applicability of an NIR sensor to characterise epithermal Au-Ag ores on their economic value. The economic value of the ore samples that were used for the testwork mainly depends on the Au grade. Ag is mined as a by-product and higher Ag grades increase ore value. Relatively high concentrations of carbonaceous materials or sulphide minerals on the other hand decrease ore value because these lower the recovery of Au and Ag during ore processing. The objectives of the testwork were therefore to investigate if an NIR sensor can be used to distinguish i) ore particles with low Au and Ag grades, ii) ore particles with high carbon contents, iii) ore particles with high sulphide contents.

4 Methods – Test work approach

The test work included NIR spectroscopic measurements on 94 samples that originate from a South-American mine. This mine exploits a high-

sulphidation epithermal Au-Ag deposit. Each sample is a rock particle of about 5-15 cm in diameter. The sample set consists of 80 samples that were collected from the ore zone of the deposit and 14 samples that were collected from an unmineralised zone. These different zones are defined by the geological deposit model that is used by the mine. The subsets were selected at random from two locations that were about 250 m apart.

7 NIR reflection spectra were measured on each sample with an ASD Fieldspec3 portable spectroradiometer. This device records reflected NIR radiation at wavelengths ranging from 350 to 2500 nm. For analysis of the measured NIR spectra, this wavelength range was subdivided into two regions. This was done because two different types of absorption processes take place in these regions. At wavelengths ranging from 350 to 1300 nm the measured NIR spectra are dominated by charge transfer absorptions of the Fe-ion (Fe2+ and Fe3+). These absorptions therefore allow determination of Fe-bearing mineralogy. This wavelength region will be referred to as the visible (VIS) region of the NIR spectra. At wavelengths ranging from 1300 to 2500 nm the measured NIR spectra are dominated by absorptions from molecule bond vibrations. These absorptions allow determination of hydrothermal alteration mineralogy. This wavelength region will be referred to as the short wave infrared (SWIR) region of the NIR spectra.

The NIR active mineralogy was determined from each measured NIR spectrum by comparing the spectra with reference spectra from the GMEX spectral interpretation field manual [16] and the USGS spectral library [17]. X-ray diffraction (XRD) was performed on a subset of 36 samples to validate the determined NIR active mineralogy. Selection of this subset was based on a classification of samples on the NIR spectra. Fire assay was performed on the samples in the subset to determine their Au and Ag grades. Carbon and sulphur contents of samples were determined by using a LECO analyser [18].

5 Methods – Classification with Partial Least Squares Discriminant Analysis (PLS-DA)

A classification model known as partial least squares discriminant analysis (PLS-DA) was applied to investigate the potential of using the NIR

spectral data to distinguish between pre-defined groups of samples. PLS-DA is based on partial least squares (PLS) regression [19]. This is a method that is used for calibrating a multivariate linear prediction model [20,21]. PLS regression hereby allows investigating the possibilities of predicting a set of response variables from a large set of predictor variables. A detailed description of PLS regression is presented by Wold et al. [21] and Abdi [22].

The difference between PLS-DA and PLS regression is that instead of predicting one or more dependent variables, PLS-DA is used to predict a certain class analogy. This is performed by simply calibrating a PLS regression model in which the set of response variables is replaced by a dummy matrix with assigned class memberships [19]. The advantage of PLS-DA over most other classification models is that PLS-DA does not only relate the predictor data to class membership, it also models the common structure between these datasets. This is achieved by finding a set of latent variables (LVs) that describe maximum covariance between the predictor and class data [21,22]. By using the LVs, the model is able to handle numerous and collinear predictor variables [21]. This was considered an advantage for making classification models based on the NIR spectral data, since this type data can be correlated and noisy.

PLS-DA was performed on individual NIR spectral measurements. 7 measured spectra on each individual sample were used for this. To calibrate the PLS-DA models, the spectra were assigned to the class that the sample belongs to. Only two different classes were used in each PLS-DA model. Definition of the classes was based on the sorting objectives stated in section 3. The PLS-DA model predicts a response for each measured spectrum. Responses for samples were calculated by averaging the responses that resulted for the individual measurements. By applying a threshold to these averaged responses, classification of samples was performed. Apart from the responses, PLS-DA also calculates loadings and scores. The loadings contain information on the wavelength regions that are important for classification into the classes [21,22]. The scores describe the relationship between these loadings and the measured spectra.

PLS-DA was applied to the VIS region (400 – 1300 nm) and the SWIR region (1300 – 2500 nm) of the NIR spectra separately. The spectra on the SWIR region were hull quotient corrected before applying the PLS-DA. This type of correction removes the overall reflection of the NIR spec-

tra, so that only the absorption features that are produced by molecule bond vibrations remain [10]. This is necessary to ensure that the model only uses the features that relate to mineralogy to perform the classification. The spectra on the VIS region were not corrected. This was not needed because the charge transfer absorptions that occur in this region dominate the overall reflection of the spectrum.

When using PLS-DA, it is important to select the optimal number of LVs that are used by the model. A higher number of LVs increase the accuracy of the model on data used for calibration, but the predictive power on other data may be decreased due to 'overfitting' [21, 22]. To select the optimal number of LVs, only 75 percent of the samples were used for model calibration. The remaining samples were used to validate the resulting classifications. The error rate of classification versus the number of LVs was calculated for 100 randomly chosen calibration and validation subsets. The number of LVs at which the lowest average error rate resulted for the validation subset was selected for creating the PLS-DA classification model.

The PLS-DA was performed with algorithms from the classification toolbox for Matlab from the Milano Chemometrics and QSAR Research Group [23]. Before applying the PLS-DA the data was mean-centered.

6 Results – Mineralogy determined with NIR spectroscopy

Figure 1 presents an overview of measured NIR spectra of all the different minerals that were determined on the samples with NIR spectroscopy. The minerals determined from the VIS region of the NIR spectra are presented separately of those from the SWIR region. Almost all spectra in figure 1 match those of single minerals [16,17]. Only the SWIR spectra of diaspore and dickite are mixed with other minerals. The spectrum of diaspore in figure 1 shows additional features by pyrophyllite around 1400 and 2170 nm. The presented spectrum of dickite is actually dominated by broad water absorptions that occur around 1400 and 1940 nm. Dickite was determined from the small absorption features that occur at 1380, 1415, 2175 and 2205 nm. The spectrum of water that is presented in figure 1 is likely produced by small fluid inclusions in quartz. The occurrence of quartz with fluid inclusions is common at ep-

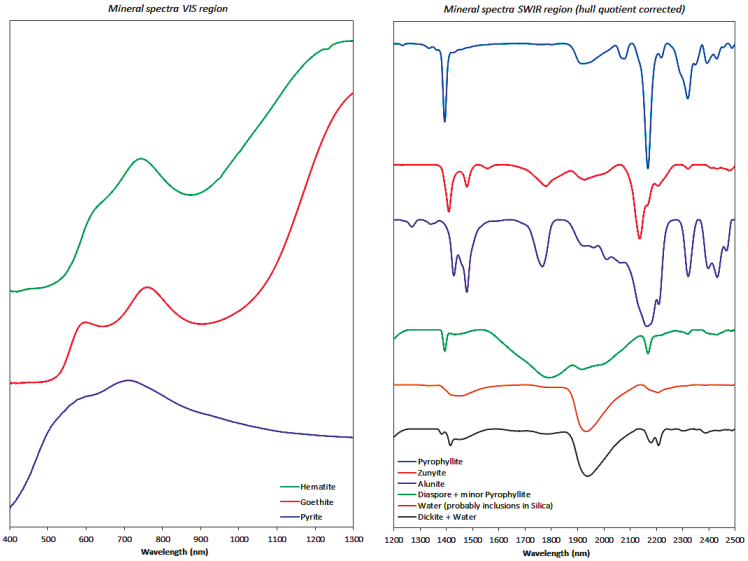

Figure 16.1: Measured NIR spectra of identified minerals

ithermal deposits [13] and was validated by XRD. It was made sure that all samples were dry while taking the measurements.

The SWIR region of the measured NIR spectra often contains absorptions by 2 or 3 different minerals. The VIS region on the other hand only shows a dominant mineralogy because all the characteristic mineral absorptions overlap. A fraction of the measured VIS spectra also had no characteristic shape at all, indicating an absence of significant amounts of Fe-bearing minerals. In total, 22 different combinations of NIR active mineral assemblages were determined from the samples. Minerals that were most often identified include pyrophyllite, quartz (water spectrum), hematite and goethite. Diaspore and zunyite were often determined from mixed spectra with pyrophyllite. Dickite always occurred together with quartz.

Apart from the spectra in figure 1, also spectra with a very low reflection over the entire VIS and SWIR spectral ranges were measured. It resulted that these spectra are representative for the carbonaceous ore

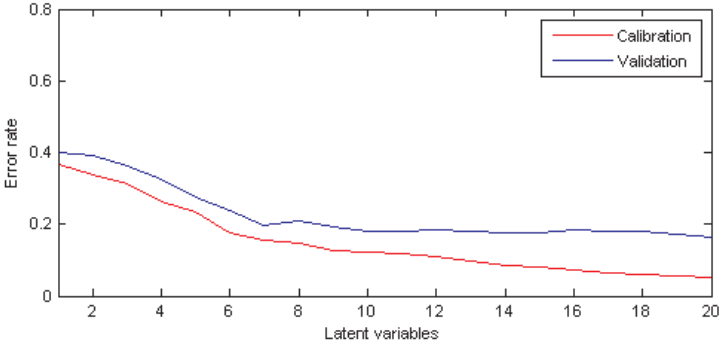

Figure 16.2: Error Rate vs. nr of Latent Variables in PLS-DA

materials. The low reflection of carbonaceous samples is also observed visually from their dark black colour.

XRD validated the occurrence of almost all minerals that were identified with NIR spectroscopy. The only mineral that was not validated by XRD is dickite. However, it is possible that the weight fraction of dickite in the samples is below the limit of detection of XRD. The NIR spectra from which dickite was identified also showed only weak absorption features of this mineral, indicating relatively low concentrations.

7 Results – Classification model for sorting on Au

Different PLS-DA classification models have been produced to classify the samples on the sorting objectives stated in section 3. This section presents an overview of the results from a PLS-DA model that was aimed at distinguishing samples with Au grades < 0.20 ppm. Processing of ore samples below this grade is not profitable. The classification was performed on the SWIR region of the spectra.

The first step in the PLS-DA classification was to select the optimal nr of LVs that are used by the model. This was performed by calculating the error rate of classification versus the number of LVs for 100 randomly chosen calibration and validation subsets. Figure 2 presents

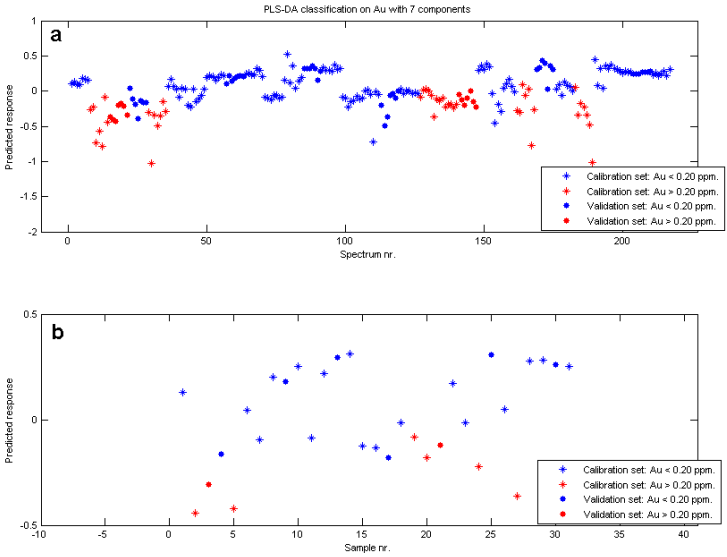

Figure 16.3: Predicted responses from PLS-DA

the average of these classifications. This figure shows that there is no significant decrease in the error rate of the validation subset when more than 7 LVs are used. 7 LVs were therefore selected for performing the PLS-DA classification.

Figure 3a presents the responses that the PLS-DA model calculated for each measured SWIR spectrum. The different colours in this figure refer to the different classes on which the model was calibrated. The calibration of the model is performed in such a way that the difference between the predicted responses of the two classes is maximised. Figure 3b shows the sample responses, which were calculated by averaging the responses of the SWIR spectra that were measured on each sample. The stars and dots in figure 3a and 3b refer to samples that were used for calibration and validation of the model. The figures show that for each class the responses of the validation subset fall within the range of responses of the calibration subset. The classification results are therefore consistent for samples that were not included during model calibration.

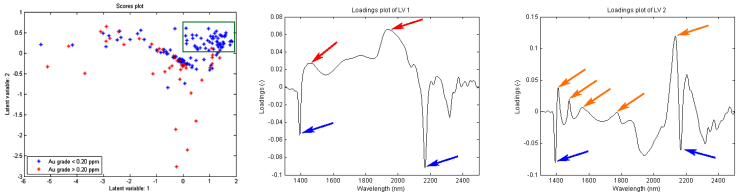

Figure 16.4: Scores and Loadings from PLS-DA

Using different calibration and validation subsets produced similar results.

Figure 3b shows that there is overlap between the predicted responses of the two classes. However, it also shows that calculated responses $>$ -0.05 only result on samples with low Au grades. By applying a threshold to the responses it is therefore possible to distinguish a group of samples that all have Au grades < 0.20 ppm. To investigate which SWIR spectral features allow identification of these samples, the scores and loadings of the model were analysed.

Figure 4 presents the scores and loadings for the first two LVs that are used by the PLS-DA model. The green rectangle indicates a region on the score plot where only measurements on low grade samples result. The first loadings plot shows that these measurements can be distinguished on the basis of absorption features relating either to water (red arrows) or pyrophyllite (blue arrows). The second loadings plot shows that the distinction between spectra is also based on the occurrence of either pyrophyllite (blue arrows) or zunyite (orange arrows). The scores of the low grade samples in the green rectangle are positive on both the 1st and 2nd LV. This relates to NIR spectra that are represented by absorption features in the negative direction of the loadings of both LVs. It results that low grade samples can be identified from the occurrence of spectral features relating to pyrophyllite and absence of features relating to water (quartz) and zunyite. Investigation of scores and loadings of other LVs of the model also showed that features relating to diaspore are characteristic for the low grade samples. These results were confirmed by visual interpretation of the spectra and the determinations of mineralogy that resulted from XRD.

Table 1: Geochemistry of samples with pyrophyllite & no zunyite (Class 1) and other samples (Class 2)

Averages before classification		Averages Class 1 (45 %)		Averages Class 2 (55 %)	
Au (ppm)	0.261	Au (ppm)	0.086	Au (ppm)	0.405
Ag (ppm)	1.594	Ag (ppm)	0.000	Ag (ppm)	2.906
As (%)	0.007	As (%)	0.002	As (%)	0.011
C (%)	0.002	C (%)	0.000	C (%)	0.004
S (%)	0.758	S (%)	0.721	S (%)	0.788

Table 2: Geochemistry of samples with carbon (Class 2) and other samples (Class 1)

Averages before classification		Averages Class 1 (86 %)		Averages Class 2 (14 %)	
C (%)	0.722	C (%)	0.002	C (%)	5.186
Au (ppm)	0.239	Au (ppm)	0.261	Au (ppm)	0.104
Ag (ppm)	1.644	Ag (ppm)	1.594	Ag (ppm)	1.960
As (%)	0.007	As (%)	0.007	As (%)	0.006
S (%)	0.938	S (%)	0.758	S (%)	2.052

Table 3: Geochemistry of samples with pyrite (Class 2) and other samples (Class 1)

Averages before classification		Averages Class 1 (71 %)		Averages Class 2 (29 %)	
Au (ppm)	0.261	Au (ppm)	0.313	Au (ppm)	0.132
Ag (ppm)	1.594	Ag (ppm)	2.245	Ag (ppm)	0.000
As (%)	0.007	As (%)	0.009	As (%)	0.001
C (%)	0.002	C (%)	0.003	C (%)	0.000
S (%)	0.758	S (%)	0.190	S (%)	2.147

Figure 16.5: Sample classification based on mineralogy detectable with NIR spectroscopy

8 Results – Overview of classification results

The previous section presented an example of how PLS-DA was used to identify certain minerals from the SWIR spectra that are characteristic for samples with Au grades < 0.20 ppm. The same method was applied to other Au grades and the carbon and sulphur content of samples. Also the VIS region of the measured spectra was investigated by using the same approach. Based on the information that this provided, certain assemblages of NIR active minerals could be defined that only occur on samples with Au, C or S grades within a certain range. Figure 5 presents the results of three classifications that were based on distinguishing samples that contain these mineral assemblages. PLS-DA modelling showed it was possible to make this distinction on the basis of NIR spectral data.

The classification result in table 1 is based on distinguishing samples that contain pyrophyllite while zunyite is absent. The table shows

significant differences between the average Au and Ag grades of both sample groups. The maximum Au and Ag grades of group 1 are furthermore 0.19 and 0.00 ppm. It results that the NIR sensor can be used to distinguish a fraction of the sub-economic ore samples. However, it should be noted that it is unknown how well these samples represent the entire ore deposit.

The classification result in table 2 is based on distinguishing samples with a low overall reflection. The samples that contain carbon generally absorb most of the NIR radiation which is also visible from their dark black colour. Classifying the NIR spectra on the average reflection therefore allows distinguishing carbonaceous ore samples.

The classification result in table 3 is based on distinguishing samples of which the VIS spectra are characteristic for pyrite. VIS spectra of samples in group 1 either showed Fe-oxide minerals or no diagnostic mineral absorptions. By distinguishing samples containing NIR active pyrite, significant differences between the average sulphur content of both sample groups results.

9 Conclusions

The following conclusions were drawn from the testwork

- It is possible to use NIR spectroscopy to distinguish ore samples with low Au and Ag grades. This is based on specific alteration mineral assemblages detectable from the SWIR region of the NIR spectra (1300 – 2500 nm).
- The average NIR reflection of samples can be used to distinguish samples with relatively high C contents. This distinction can also be made visually because carbonaceous samples have a dark black colour.
- It is possible to use NIR spectroscopy to distinguish between samples with high and low S contents. This is based on detecting either Fe-oxide or Fe-sulphide minerals from the VIS region of the NIR spectra (350 – 1300 nm).
- PLS-DA is an effective technique to investigate classification possibilities based on NIR spectroscopic data.

References

1. J. Salter and N. Wyatt, "Sorting in the minerals industry: past, present and future," in *Minerals Engineering, 4*, 1991.
2. R. Sivamohan and E. Forssberg, "Electronic sorting and other preconcentration methods," in *Minerals Engineering, 4*, 1991.
3. H. Wotruba and F. Riedel, "Ore preconcentration with sensor based sorting," in *Aufbereitungs technik,46(5)*, 2001.
4. M. Dalm, M. Buxton, J. van Ruitenbeek, and J. Voncken, "Application of near-infrared spectroscopy to sensor based sorting of a porphyry copper ore," in *Minerals Engineering 58*, 2014.
5. M. Buxton and J. Benndorf, "The use of sensor derived data in optimization along the mine-value-chain," in *International congress of the ISM*, Clausthal-Zellerfeld, 2013a.
6. ——, "The use of sensor derived data in real time mine optimization: A preliminary overview and assessment of techno-economic significance," in *Proceedings of the 2013 SME Annual Meeting*, 2013b.
7. H. Harbeck and H. Kroog, "New developments in sensor based sorting," in *Aufbereitungstechnik, 49(5)*, 2008.
8. J. Bergmann, "Sensor based sorting," in *Industrial Minerals*, July 2011.
9. G. Hunt, "Spectral signatures of particulate minerals in the visible and near infrared," in *Geophysics 42(3)*, 1977.
10. R. Clarck, "Spectroscopy of rocks and minerals and principles of spectroscopy," in *Manual of remote sensing, remote sensing for the earth sciences, vol. 3*, 1999.
11. A. Thompson, P. Hauff, and A. Robitaille, "Alteration mapping in exploration: application of short-wave infrared (swir) spectroscopy," in *Society of Economic Geologists Newsletter, 39*, 1999.
12. N. White and J. Hedenquist, "Epithermal gold deposits: styles, characteristics and exploration," in *Society of Economic Geologists Newsletter, 23*, 1995.
13. S. Simmons, N. White, and D. John, "Geological characteristics of epithermal precious and base metal deposits," in *Economic geology, 100th anniversary volume*, 2005.
14. R. Sillitoe, "Epithermal models: genetic types, geometrical controls and shallow features," in *Mineral deposit modelling*, 1993.
15. F. Pirajno, "Hydrothermal mineral deposits, principles and fundamental concepts for the exploration geologist," 1992.

16. AusSpec, "G-mex spectral interpretation field manual," AusSpec International ltd., 2008.
17. R. Clark, G. Swayze, R. Wise, E. Livo, T. Hoefen, R. Kokaly, and S. Sutley, "Usgs spectral library splib06a: U.s. geological survey, digital data series 321," [online] http://speclab.cr.usgs.gov/spectral-lib.html, 2007.
18. LECO, "Leco carbon/sulphur analyzers," [online] http://www.leco.com/products/analytical-sciences/carbon-sulfur-analyzers, 2015.
19. M. Sjostrom and S. Wold, "Pls discriminant plots," in *Pattern recognition in practice II*, 1986.
20. T. Naes and H. Martens, "Multivariate calibration ii. chemometric methods," in *Trends in analytical chemistry, 3(10)*, 1984.
21. S. Wold, M. Sjostrom, and L. Eriksson, "Pls-regression: a basic tool of chemometrics," in *Chemometrics and intelligent laboratory systems,58*, 2001.
22. H. Abdi, "Partial least squares regression and projection on latent structure regression (pls regression)," in *Wiley interdisciplinary reviews: computational statistics, 2(1)*, 2010.
23. D. Ballabio, "Classification toolbox," [online] http://michem.disat.unimib.it/chm/download/softwares.htm, 2013.